International Journal of Pharmaceutics 369 (2009) 155–161

Contents lists available at ScienceDirect

International Journal of Pharmaceutics

journal homepage: www.elsevier.com/locate/ijpharm

Pharmaceutical Nanotechnology

DNA loaded carrier preferential extravasation from tumor blood vessel

Ge Jiang[a,1], Yingzhi Jiang[b,1], Yuanyuan Shen[c], Kweon-Ho Nam[d], Donhaeng Lee[e], Zhonggao Gao[c,d,*]

[a] Key Laboratory of Bio-organic Chemistry and College of Bioengineering, Dalian University, Dalian 116622, China
[b] College of Pharmacy, Yanbian University, Yanji 133000, China
[c] Chinese Academy of Medical Sciences and Peking Union Medical College, 1 Xian Nong Tan Street, Beijing 100050, China
[d] Department of Bioengineering and Pharmaceutics, University of Utah, Salt Lake City, UT 84112, USA
[e] Inha University Hospital, Incheon, Republic of Korea

ARTICLE INFO

Article history:
Received 27 June 2008
Received in revised form 20 October 2008
Accepted 20 October 2008
Available online 5 November 2008

Keywords:
DNA delivery
Polymethacrylic acid
Dorsal skin fold window chamber
Cancer cells

ABSTRACT

Non-viral gene delivery carriers were prepared by using DNA/polyethylenimine/polymethacrylic acid (DPP) polyplexes and its extravasation from tumor blood vessel was evaluated with mouse dorsal skin fold window chamber model. The DNA/PEI (DP) complex with a ratio of N to P (10/1) was coated with polymethacrylic acid, and the ratio of PMA to DNA complex in DNA/PEI/PMA (DPP) polyplex was fixed 0.03 (w/w). The surface charges of the DP and DPP polyplex were positive 26 and 15, respectively. The size of DP and DPP polyplex were 161 nm and 195 nm. The transfection efficiencies in HepG2 cells were about 30-fold and 20-fold higher than that in HeLa and L/C cells in the presence of 50% serum, respectively. The DPP polyplex showed a reduced erythrocyte aggregation activity and a decreased cytotoxicity in cancer cells. After being incubated 30 min, Fluorescently labelled DPP polyplex uptaken by cancer cells decreased, compared with DP by measuring flowcytometry. DPP polyplex penetrating through tumor blood vessel appeared fast and stayed longer in tumour interstitial, this fact was observed from mouse dorsal skin fold window chamber model.

Published by Elsevier B.V.

1. Introduction

Efficient delivery of DNA into mammalian cells is critical for gene therapy and gene regulation studies. Substantial efforts have been focused on the development of non-viral vectors such as cationic liposomes and polymers due to the severe side effect of using viral vector. Since polyethylenimine (PEI) is stable, economic, easy to manipulate, it has gained much attention as a gene delivery vehicle it. The main use of PEI in DNA delivery is for condensing linear structure of DNA to tiny sphere structure via negative and positive electrostatic reaction to payload into gene delivery carrier. Although PEI is one of the most efficient non-viral vectors, its use for gene delivery has been limited by cytotoxicity and lower efficiency in the presence of serum. It is reported that the PEI is inherent cytotoxicity with the endosomolytic activity via buffering capacity at the acidic endosomal pH (Boussif et al., 1995, 1996) and interaction between the polymer and serum proteins in the blood components (Chollet et al., 2002). Ahn (Ahn et al., 2002), Tseng and Jong (2003) reported that the PMA could reduce the cytotoxicity of PEI and improve its solubility. Oupicky (Oupicky et al., 2002) and Trubetskoy's group (Trubetskoy et al., 2003) developed a PMA coated gene delivery carrier for preventing undesirable interaction via binding to serum protein and lower cytotoxicity *in vivo*. Therefore, PMA as a synthetic hydrophilic polyanions could reduce the PEI reaction with blood serum *in vivo* and is expected to increase the transfection efficiency in the presence of serum.

It is also reported that the synthetic anionic PMA possesses antiviral activity and is less cytotoxic (Ormai and Palkovits, 1975). In addition, the carboxyl anion of PMA has been reported to connect with highly charged polycations (Izumrudov et al., 2005), and the driving forces and the interaction between the building blocks have been studied (Sukhishvili and Granick, 2002; Xie and Granick, 2002; Kharlampieva and Sukhishvili, 2003; Yang et al., 2003). PMA has several unique properties that have enabled it to be used as a matrix for the entrapment and/or delivery of a variety of biological agents including nucleic acid (Jones et al., 2003). Nevertheless, anionic polymers based on PMA have not previously been studied for grafting on DNA/PEI (DP) complex for gene delivery to mammalian cells *in vitro* and *in vivo*.

In this study, we explored the gene delivery efficiency of PMA coated DNA/PEI polyplex to cancer cells in terms of cytotoxicity, transfection in the presence of serum protein, and extravasation from tumor blood vessel. The results showed that DNA/PEI/PMA

* Corresponding author at: Institute of Materia Medica, Chinese Academy of Medical Sciences and Peking Union Medical College, Beijing, 100050, China. Tel./fax: +86 10 63028096.
E-mail address: zggao@imm.ac.cn (Z. Gao).
[1] These two authors contributed equally to this work.

0378-5173/$ – see front matter. Published by Elsevier B.V.
doi:10.1016/j.ijpharm.2008.10.022

(DPP) significantly increased transfection efficiency, reduced the interaction with erythrocytes, and preferentially accumulated on the tumor site.

2. Materials and methods

2.1. Materials

PMA (MW 9500), fetal bovine serum (FBS) and trypsin EDTA (0.25%) were purchased from Hyclone (Logan, UT). Dulbecco's modified Engle medium (DMEM), RPMI 1640 and Dulbecco's phosphate-buffered saline (PBS) were obtained from Gibco BRL (Gaithersburg, MD) and polyethylenimine (branched, M_r = 25,000) from Aldrich (Milwaukee, WI). Luciferase assay reagent was obtained from Promega (Madison, WI). All the reagents including the reporter plasmids of pCMV-LUC were used without further purification.

2.2. Cancer cell culture

HeLa (human uterine cervical carcinoma), C/L (Chang liver, epithelial human hepatocellular carcinoma) cell, HepG2 (human hepatocellular carcinoma) cell and Normal human hepatic cell line L02 (Shanghai, China) were cultured at 37 °C in a humidified incubator containing 5% CO_2. DMEM was supplemented with 10% FBS and 10 IU/mL of antibiotics (penicillin). MCF-7 (human breast carcinoma) cell was cultured in RPMI 1640 medium supplemented with 10% FBS and 10 IU/mL of antibiotics (penicillin).

2.3. Preparation of DP complex and DPP polyplex

DP complexes were prepared by mixing 1 μg of plasmid DNA with the desired amount of PEI (1 μg of plasmid DNA contains 3 nmol of phosphate, and 1 μg of 20 mM PEI has 20 nmol of amine nitrogen), and then incubated for 10 min at room temperature. Prepared DP complexes (N/P ratio of 10) were mixed with various amounts of PMA solution (PMA/DNA weight ratio ranged from 0.003 to 0.3) and incubated for 10 min at room temperature. The resulting complexes or polyplexes were followed by the addition of diluting water to give a final NaCl concentration of 150 mM before use.

2.4. Fluorescent labeling of PEI

PEI was fluorescently labeled with the amine reactive probe, Oregon Green 488 carboxylic acid succinimidyl ester (Godbey et al., 1999). Briefly, PEI was dissolved in 0.2N sodium bicarbonate solution with the final concentration of 20 μg/L in pH 8.5. A 1-mL aliquot of PEI solution was transferred into a microcentrifuge tube, and 0.5 mL of the prepared probe (dissolved in DMSO to a final concentration of 1 mg/mL) was added. The solution, protected from light, was incubated at room temperature on an orbital plate shaker for 4 h, and subsequently stored at 4 °C.

2.5. Measurement of particle size and zeta potential of DPP polyplexes

The particle size and the surface charge of the DP or DPP polyplex were determined by dynamic light scattering (ELS-8000, Otsuka Electronics, Japan). Samples were prepared at a DNA concentration of 10 μg/mL in a volume of 500 μL, and each sample was measured in duplicates for 2 min at room temperature.

2.6. Cytotoxicity assay

The cytotoxicity of the DP complex and DPP polyplex was determined by MTT assay. HepG2 cells were seeded in 96-well plates with 5×10^3 cells/well density and incubated for 24 h. Twenty microliters of DP or DPP polyplex containing 0.2 μg of DNA was added to cells in the absence of FBS. After 24 h transfection, 20 μL of MTT solution (2 mg/mL in PBS buffer) was added and the plates were incubated for additional 4 h at 37 °C. MTT-containing medium was removed and 100 μL of DMSO was added to dissolve the formazan crystal formed by cells. The absorbance was measured at 570 nm and the cell viability (%) was calculated according to the following equation:

$$\text{cell viability}(\%) = \frac{\text{OD}_{570(\text{sample})}}{\text{OD}_{570(\text{control})}} \times 100$$

where $\text{OD}_{570(\text{sample})}$ and $\text{OD}_{570(\text{control})}$ represent the absorbance value for the wells treated with sample and PBS buffer only, respectively.

2.7. In vitro transfection test

In vitro gene transfection tests were carried out with HeLa, C/L and HepG2 cells. Cells were seeded in a 24-well plate containing 0.4 mL of DMEM with a 1×10^4 cells/well, 5×10^4 cells/well and 3×10^4 cells/well density, respectively. Medium was replaced with 0.4 mL of fresh medium containing various concentrations of FBS after 24 h incubation. The maximum FBS concentration is up to 50% in the medium. Then, each well received 100 μL of freshly prepared DP complex or DPP polyplex containing 1 μg of DNA (pCMV-Luc gene). Cells were incubated in a 5% CO_2 incubator at 37 °C for 48 h. The cells were washed twice with PBS and re-suspended in 100 μL of cell lysis reagent. The cell debris was pelleted by centrifugation at 12,000 rpm and 4 °C for 20 min. The supernatant (5 μL) was mixed with 25 μL of luciferase assay solution. Finally, the luciferase activity was measured with a luminomate (Biolumat LB 9500, Berthold, Germany).

2.8. Erythrocyte aggregation assay

Fresh blood was collected from C57/BL6 mice and immediately mixed with sodium citrate (25 mM). Erythrocytes were washed 3 times with cold Ringer solution on ice. The washed erythrocyte suspension (200 μL) was mixed with DP complex or DPP polyplex in 24-well plate (Nunc, Rochester, NY) and incubated at 37 °C for 1 h. The erythrocyte aggregation was observed with a microscope (Nikon TS100, Tokyo, Japan).

2.9. Flow cytometry

HepG2 and MCF-7 cells were cultured in 75 mm^2 cell culture flasks using DMEM and RPMI 1640 medium supplemented with 10% FBS, 0.4% nystatin, 1.2% insulin, and 1.2% penicillin–streptomycin. Medium was replaced every other day. Incubator was maintained at 5.0% CO_2 and 36.5 °C. The cells (1×10^6 cells/well) were seeded in a 6-well plate, incubated overnight and harvested by 0.2% (w/v) trypsin–0.1% (w/v) EDTA solution. Two milliliters of fluorescently labeled DP complex or DPP polyplex was introduced to each well and incubated for 30 min. The cells were trypsinized and washed 3 times with PBS solution and then fixed with 2.5% glutaradehyde. After being filtered through a nylon mesh, cell fluorescence was measured by flow cytometry (FACScan, Becton Dickinson, NJ) (Gao et al., 2004, 2005).

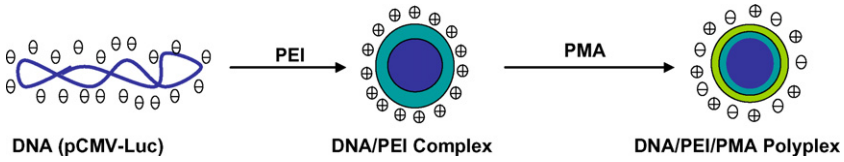

Fig. 1. The procedure of preparing DNA/PEI complex and DNA/PEI/PMA polyplex was schematically presented.

2.10. Dorsal skin fold window chamber

In order to evaluate DPP polyplexes how to overcome serum binding in blood stream, a titanium window chamber frame was implanted in the mice (Wu et al., 1993, 1997; Hobbs et al., 1998; Lichtenbeld et al., 1996; Monsky et al., 1999), animals were anesthetized with i.p. ketamine/xylazine at a dose of 100 mg/kg and 10 mg/kg of body weight. About 1 cm diameter in circle skin was removed on the left side of the flap, leaving the skin and underlying fascia tissue on the right side intact. A pair of titanium windows was mounted with an alignment of the circular wound to the window, which was covered with a glass cover slip and a retaining ring after MCF-7 (about 500 cells in 5 μL) was implanted onto the fascia. Following recovery from anesthesia and surgery, the animals were housed in an environmental chamber at 35 °C and 50% humidity, with 12 h light/12 h dark cycle and access to rodent chow and water *ad libitum*. These conditions are necessary to maintain viability of the chamber and provide a high enough temperature to facilitate tumor growth. The fluorescent light intensities of the entire selected region and representative vascular regions were measured at each serial time point. Microcirculatory parameters were analyzed by intravital fluorescence microscopy (Tozer et al., 2001; Dewhirst et al., 2002) using specially designed animal experiment Olympus microscope (Olympus BX51WI Microscope, Leeds Precision Instruments, Inc., MN).

3. Results and discussion

Although non-viral gene delivery systems have shown significant transfection efficiency *in vitro*, their applications have been hampered by limited trafficking to the target site *in vivo*, substantial decreased transfection efficiency caused by non-specific interactions with serum components (Boussif et al., 1995). We designed a novel ternary polyplex comprised of DPP in which positive charge was decreased via neutralization of positive charges of PEI with negative charges of PMA. Fig. 1 shows schematic representations for the preparation of the DP complex and the DPP polyplex. The negatively charged PMA can form a charge-mediated polyplex with the positive charged DP complex. The PMA coated DP polyplex reduced the positive charge on the surface of the DP complex and prevented its binding from blood components.

3.1. Characterization of DPP polyplex

The particle size and zeta potential of the DPP polyplexe in terms of various ratio of PMA to DP complex were summarized in Table 1. With increasing the ratio of PMA to DNA from 0.003 to 0.03 in the DPP mixture, the polyplex size decreased from 190 nm to 150 nm because neutralization of surface charge subsequently decreases the nanoparticle surface intensity. However, when the ratio of PMA to DNA was increased from 0.03 to 0.3, the polyplex size was expanded from 150 nm to 161 nm due to over distribution of negative charges on the nanoparticle surface. With increasing the ratio of PMA to DNA from 0.003 to 0.3 in the DPP mixture, the zeta potential gradually decreased due to increasing negative charges of the PMA on the nanoparticle surface. The cytotoxicity of the DPP polyplex was dramatically reduced by the coating of PMA as shown in Fig. 2. With increasing N/P ratios from 2/1 to 10/1 via increasing PEI in the DP complexes, Cytotoxicities were significantly increased because of PEI toxicity as presented in Fig. 2A. The cell viability of DPP (N/P, 10) was significantly increased ($p < 0.05$, 1.6-fold), when compared with DP (N/P, 10). The severe cytotoxicity of DP come from PEI buffering capacities between pH 7.2 and 5.0 in acidic tumor tissue, which could buffer the endosome and potentially induce its rupture (Boussif et al., 1995; Midoux and Monsigny, 1999). It is reported that the protein-expression levels mediated by the polycationic proton-sponge polymer, PEI, were at least 10-fold greater than polylysine alone (Hunter, 2006). Therefore, the PMA coated PEI could directly prevent PEI from interacting with cells, and resulted in a significant decrease in cytotoxicity. Anionic PMA

Table 1
Characterization of the DNA/PEI/PMA polyplexes contained various PMA to DNA weight ratios. The N/P ratio of PEI to DNA was fixed at 10 and the DNA concentration was 1 μg/mL ($n = 5$).

PMA/DNA (w/w)	0	0.003	0.03	0.3
Particle size (nm)	190 ± 7.67	175 ± 5.76	150 ± 6.72	161 ± 3.42
Zeta potential (mV)	26 ± 2.34	21 ± 1.56	17 ± 0.723	15 ± 1.23

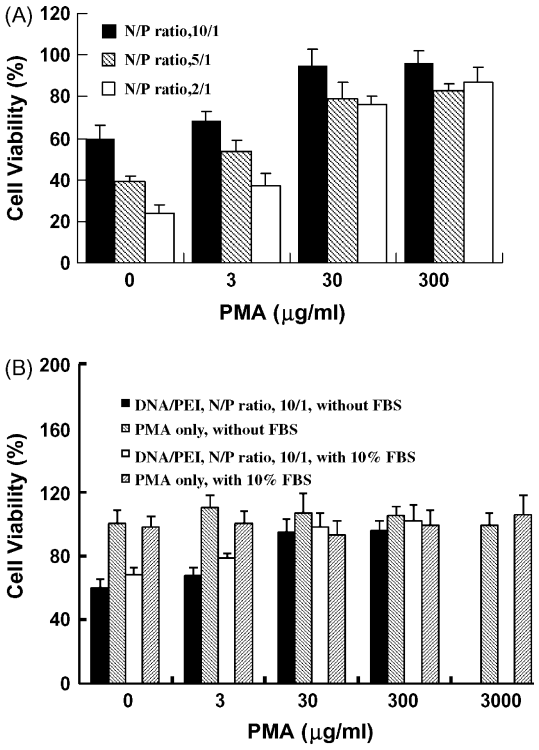

Fig. 2. Cell viabilities determined by MTT assay of Hep G2 hepatic carcinoma cells treated with various ratio of positive charge to negative charge (N/P = 10/1, 5/1, 2/1) coated with PMA (PMA to DNA ratios were from 0.003 to 0.3) (A) and treated with PMA only (B). Each experiment takes four samples ($n = 4$), and the data between different formulations were compared for statistical significance by the one-way analysis of variance (ANOVA).

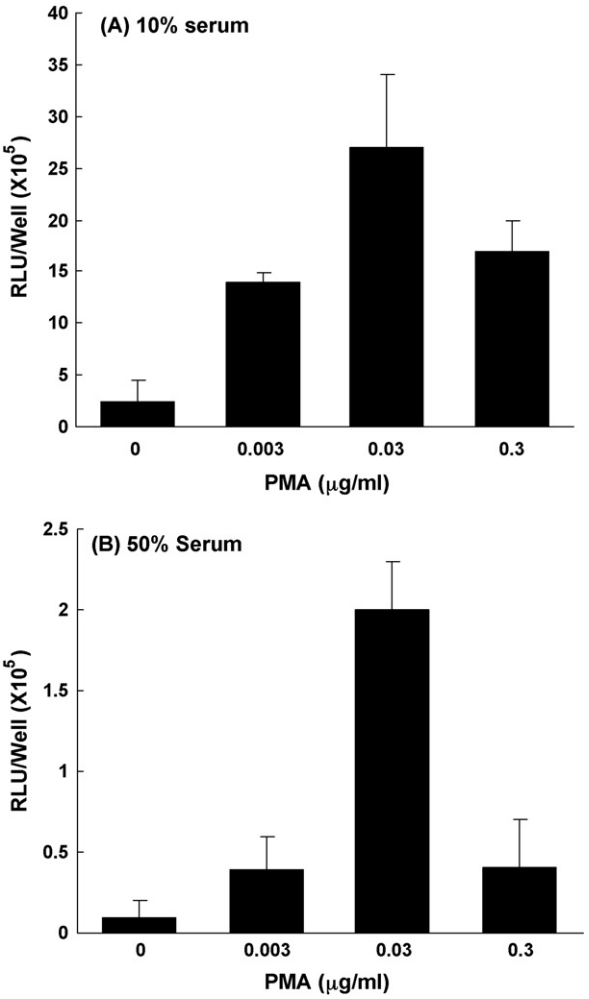

Fig. 3. Effect of PMA on the transfection efficiency of DNA/PEI (DP) complex in HepG2 hepatic carcinoma cells was presented. DP complex containing 1 μg of luciferase reporter DNA and 1.5 μL of 20 mM PEI (N/P = 10) was mixed with the indicated amount of PMA and the mixtures were transfected into HepG2 cells in the presence of 10% serum (A) and 50% serum (B). The cells were then incubated for 48 h, and the luciferase activity was measured from cell lysates (mean ± S.D., $n = 5$). The data between different formulations were compared for statistical significance by the one-way analysis of variance (ANOVA).

itself did not show any detectable cytotoxicity in the cell culture experiments as shown in Fig. 2B.

3.2. Transfection efficiency of DPP

Luciferase gene transfection efficiencies of the DPP polyplex with various ratio of PMA to DNA in HepG2 cells were shown in Fig. 3. The transfection efficiency of DPP polyplex showed 6–7-fold higher than the DPI complex in the presence of 10% serum as shown in Fig. 3A. However, the transfection efficiency of DPP polyplex was increased up to 10–15-fold compared with DP complex in the presence of 50% serum as presented in Fig. 3B. The high transfection efficiency of DPP polyplex in high serum concentration might be ascribed to the ability of the PMA providing an electrostatic stabilization to the polyplex, as previous workers demonstrated with hydrophilic polymers for example poly(acrylic acid), poly(propyl acrylic acid) and poly(*N*-2-hydroxypropyl methacrylamide) (Oupicky et al., 2002; Trubetskoy et al., 2003; Ormai and Palkovits, 1975). At the point of the ratio of PMA to DNA 0.03 in the DPP polypex regardless of serum concentration as shown in Fig. 3A and B, trasfection efficiency of DPP polyplex became maximum due to minimum particle size with suitable surface charges. The transfection efficiency of DPP (N/P, 10) was significantly increased ($p < 0.001$; $n = 3$), when compared with DP (N/P, 10) in the presence of 50% FBS as shown in Fig. 3B. In addition, the polymethacrylic nanoparticle was effectively deposited in hepatic tumor site from bloodstream (Rolland et al., 1989).

Fig. 4 shows the transfection efficiency of the DPP polyplex with different hepatic cells (HepG2, C/L cells) and HeLa cells in the presence of 10% and 50% serum. Transfection efficiencies of DP and DPP with two different hepatic cells and HeLa cells in the presence of 10% serum were similar as shown in Fig. 4A. However, transfection efficiencies of DPP with Hep G2 and L/C hepatic cells in the presence of 50% serum were 20–30-fold higher ($p < 0.001$; $n = 3$) compared with DP complex as presented in Fig. 4B. The transfection efficiency of two hepatic cells Hep G2 and L/C in the presence of 50% serum were significantly increased ($p < 0.001$; $n = 3$), when compared with HeLa cells. Fig. 4 indicates the variety of cellular pathways and processes that may be affected by the variations in gene expression. HeLa cells show low gene expression compared with Hep G2 and C/L hepatic cells, probably those hepatic cells possess high affinity protein such as apolipoprotein B which is produced primarily in human liver is much more pronounce with the polyethylenimine/polymethacrylic acid based polyplexes compared with HeLa cells. It was indicated that the PMA coated DPP polyplex could efficiently target Hep G2 and L/C hepatic tumor *in vivo* with high transfection efficiency.

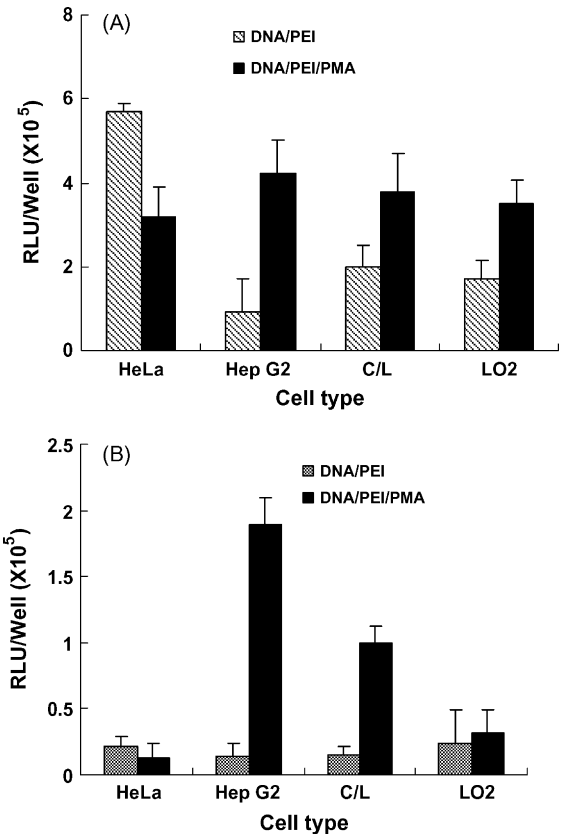

Fig. 4. The transfection efficiency of DNA/PEI/PMA (DPP) complex in HeLa, C/L and HepG2 cells were presented. DP complex containing 1 μg of luciferase reporter DNA and 1.5 μL of 20 mM PEI (N/P = 10) were mixed with the indicated 0.03 μg of PMA and the mixtures were added into total volume 1 mL in the presence of 10% (A) and 50% (B) serum medium, respectively. The cells were then incubated for 48 h, and the luciferase activity was measured from cell lysates (mean ± S.D., $n = 5$). The data between different formulations were compared for statistical significance by the one-way analysis of variance (ANOVA).

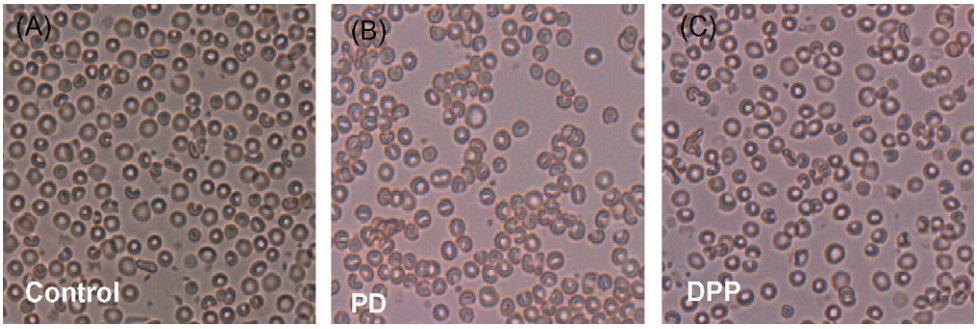

Fig. 5. The effects of PMA on the interaction of DP (PEI/DNA, N/P 10) complexes with erythrocytes in the plasma were presented: untreated erythrocytes as a control (A); treated with DP (DNA/PEI, N/P 10) (B); treated with DPP (PMA coated PD, N/P 10) (C).

3.3. DPP interaction with erythrocytes

In order to investigate the interaction of the DPP polyplex with erythrocytes, an erythrocyte aggregation assay was performed as described in previous work (Jones et al., 2003). Fresh mouse erythrocytes were incubated with either DP complex, or DPP polyplex, or PBS alone as a control as shown in Fig. 5. There was no aggregation between the erythrocyte cells in the control (Fig. 5A). However, a severe aggregation of the erythrocytes occurred by addition of DP complex because electrostatic interaction takes place between erythrocytes, as indicated by the arrows in Fig. 5B. Furthermore, when cells were incubated in the presence of a DPP polyplex with a PMA to DNA weight ratio of 0.03, the aggregation level was drastically reduced as presented in Fig. 5C. The anionic and hydrophilic nature of PMA appeared to prevent the non-specific interaction of the DP complex with erythrocytes, resulting in reducing erythrocyte aggregation, which may eventually contribute DPP polyplex to accessing the targeting site in the presence of blood serum *in vivo*.

3.4. DPP uptake by cancer cells

HepG2 and MCF-7 cancer cells were incubated in pH 7.4 DMEM and RPMI 1640 media with DP complex and DPP polyplex. The fluorescence histogram of the cellular uptake of DP complex and DPP polyplex was presented in Fig. 6. Although it was not very clear whether the polyplexes bound to cell surface or internalized by cells, all cell population-profiles were unimodal and the profiles were shifted to higher fluorescence intensity region when the cells were treated with fluorescently labeled DP or DPP. The fluorescence intensity of the cells treated with DP appeared approximately 1.2-fold and 1.5-fold higher than DPP in HepG2 and MCF-7 cells, respectively, which confirmed the higher positive charges were in DP complex surface, the more uptake by cancer cells *in vitro*, cause for severe cytotoxicity. It is demonstrated that PMA coated DP could reduce surface charges of DP nanoparticles and decrease PEI interaction with cells resulting in decreasing cell uptake as shown in Fig. 6. Higher transfection efficiency with lower cellular uptake with DPP compared with DP was mostly due to high cell toxicity from PEI in DP. As shown in Fig. 2, the cell viability was about 40% with DP compared with 80% with DPP. It was demonstrated that the cell apoptosis occurred before gene transfection with DP and led to relatively high transfection efficiency with DPP.

3.5. DPP extravasation from tumor blood vessel

The extravasation of fluorescently labelled DPP from tumor blood vessels can be visualized in the window chamber by an intravital fluorescent microscope (Wu et al., 1993; Yuan et al., 1994). Cancer cells that were implanted into mouse window chamber is shown in Fig. 7a. Blood vessel developments on days 15 in the window chamber after being implanted the cancer cells are shown in Fig. 7b. The fluorescence was confined to the vessels in normal tissue as seen after intravenous injection of DPP nanoparticles through the mice tail vein. DPP nanoparticles extravasation from normal blood vessels was limited at two initial time points (5–60 min) as shown in Fig. 7c and d. The endothelial cells of the blood vessels in normal tissue are joined by tight junctions that prevent penetration of nanoparticulates. In contrast, tumors are characterized by a defective vasculature with large gaps between the endothelial cells that allow the extravasation of nanoparticles up to 750 nm in size (Hobbs et al., 1998; Campbell, 2006). This permeability allows for accumulation of DPP particles in the tumor interstitium via the enhanced permeability and retention effect (Gao et al., 2002; Shan et al., 2006; Bartlett et al., 2007).

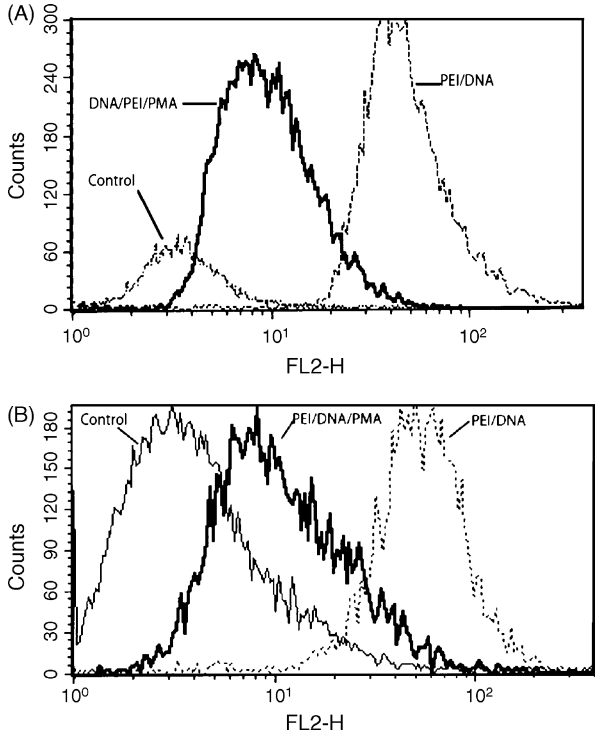

Fig. 6. Fluorescence histograms of hepatic cells HepG2 (A) and breast cancer MCF-7 cells (B) incubated with DP and DPP nanoparticles. Two milliliters fluorescence labeled DP (DNA/PEI) complex or DPP (DNA/PEI/PMA) polyplex with a 2-μg DNA concentration in medium was introduced to each well and incubated for 30 min. The cells were trypsinized and washed 3 times with PBS solution and then fixed with 2.5% glutaradehyde.

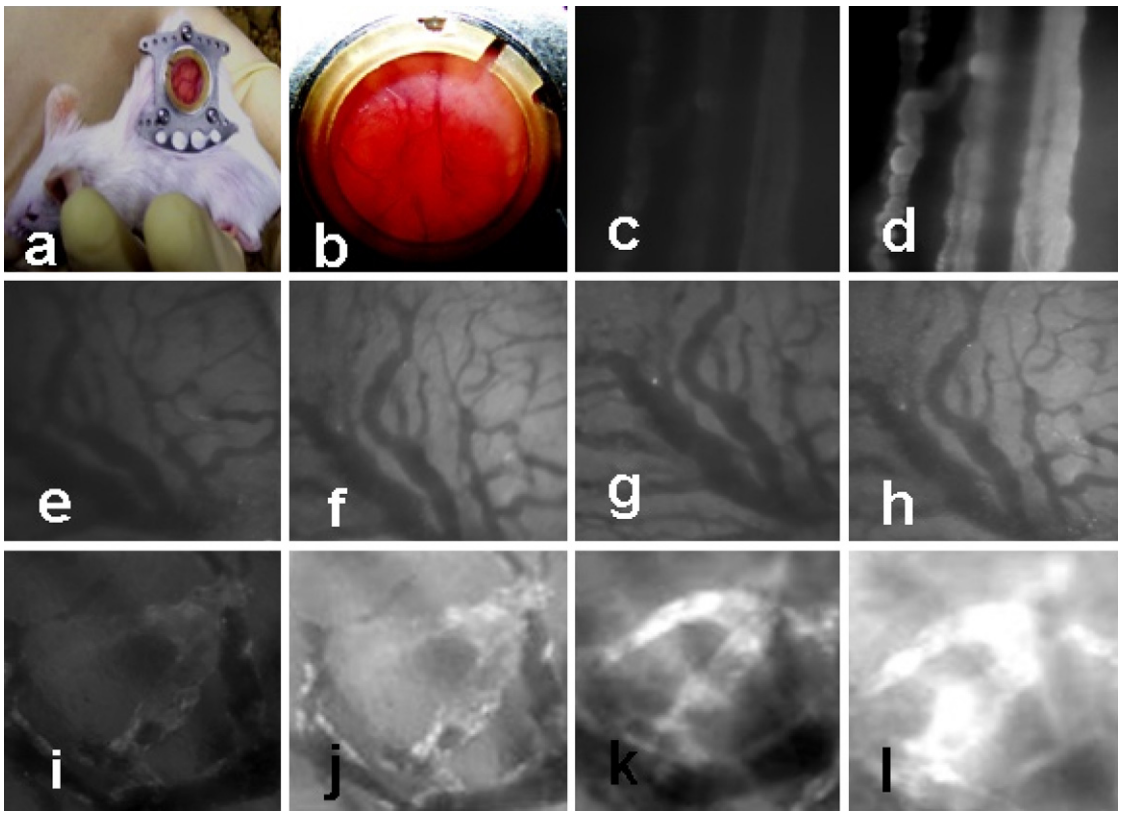

Fig. 7. Mouse dorsal skin fold window chamber made of two symmetrical titanium frames. Cancer cells were inoculated into mouse window chamber (a). After implanting MCF-7 breast cancer cells, tumor blood vessels were growing in the window chamber for 15 days (b). Normal blood vessel images after i.v. injection of DPP at 5 min and 60 min were shown (c) and (d), respectively. The tumor blood vessels after i.v. injection of DP and DPP at the time course for 60 min were present in (e: 5 min; f: 10 min; g: 30 min; h: 1 h) and (i: 5 min; j: 10 min; k: 30 min; l: 1 h). The tight junctions between cells in endothelial lining of the blood vessels in normal tissues do not allow extravasation of DPP nanoparticles. In contrast, tumors are characterized by defective vasculature with large gaps between the endothelial cells, which allows extravasation of DPP nanoparticles resulting in their accumulation in the tumor interstitium.

4. Conclusion

The DPP nanoparticles showed preferential drug accumulation in the tumor was most probably by combined effects of a long circulation time in the blood stream preventing from aggregation with erythrocytes. However, the accumulation of DP complex in the tumor site shows much less, compared with the DPP due to binding with serum in the blood stream. The enhanced bioavailability of DPP to the tumor cells resulted in improved efficacy.

Acknowledgement

This research was supported by part of National Nature Science foundation of China (No. 30873168).

References

Ahn, C.H., Chae, S.Y., Bae, Y.H., Kim, S.W., 2002. Biodegradable poly(ethylenimine) for plasmid DNA delivery. J. Control. Release 80, 273–282.
Bartlett, D.W., Su, H., Hildebrandt, I.J., Weber, W.A., Davis, M.E., 2007. Impact of tumor-specific targeting on the biodistribution and efficacy of siRNA nanoparticles measured by multimodality *in vivo* imaging. Proc. Natl. Acad. Sci. U.S.A. 104, 15549–15554.
Boussif, O., Lezoualc'h, F., Zanta, M.A., Mergny, M.D., Scherman, D., Demeneix, B., Behr, J.P., 1995. A versatile vector for gene and oligonucleotide transfer into cells in culture and *in vivo*: polyethylenimine. Proc. Natl. Acad. Sci. U.S.A. 92, 7297–7301.
Boussif, O., Zanta, M.A., Behr, J.P., 1996. Optimized galenics improve in-vitro gene-transfer with cationic molecules up to 1000-fold. Gene Ther. 3, 1074–1080.
Campbell, R.B., 2006. Tumor physiology and delivery of nanopharmaceuticals. Anti-cancer Agents Med. Chem. 6, 503–512.
Chollet, P., Favrot, M.C., Hurbin, A., Coll, J.L., 2002. Side-effects of a systemic injection of linear polyethylenimine–DNA complexes. J. Gene Med. 4, 84–91.
Dewhirst, M.W., Shan, S., Cao, Y., Moeller, B., Yuan, F., Li, C.Y., 2002. Intravital fluorescence facilitates measurement of multiple physiologic functions and gene expression in tumors of live animals. Dis. Markers 18, 293–311.
Gao, Z., Fein, H.D., Rapoport, N., 2005. Controlled and targeted tumor chemotherapy by micellar-encapsulated drug and ultrasound. J. Control. Release 102, 203–222.
Gao, Z., Fein, H.D., Rapoport, N.Y., 2004. Ultrasound-triggered targeting of micellar-encapsulated drugs to ovarian carcinoma tumors *in vivo*. Mol. Pharm. 1, 317–330.
Gao, Z., Lukyanov, A.N., Singhal, A., Torchilin, V.P., 2002. Diacyllipid-polymer micelles as nanocarriers for poorly soluble anticancer drugs. Nano Lett. 2, 979–982.
Godbey, W.T., Wu, K.K., Mikos, A.G., 1999. Tracking the intracellular path of poly(ethylenimine)/DNA complexes for gene delivery. Proc. Natl. Acad. Sci. U.S.A. 96, 5177–5181.
Hobbs, S.K., Monskey, W.L., Yuan, F., Roberts, W.G., Griffith, L., Torchilin, V.P., Jain, R.K., 1998. Regulation of transport pathways in tumor vessels: role of tumor type and microenvironment. Proc. Natl. Acad. Sci. U.S.A. 95, 4607–4612.
Hunter, A.C., 2006. Molecular hurdles in polyfectin design and mechanistic background to polycation induced cytotoxicity. Adv. Drug Deliv. Rev. 58, 1523–1531.
Izumrudov, V.A., Kharlampieva, E., Sukhishvili, S.A., 2005. Multilayers of a globular protein and a weak polyacid: role of polyacid ionization in growth and decomposition in salt solutions. Biomacromolecules 6, 1782–1788.
Jones, R.A., Cheung, C.Y., Black, F.E., Zia, J.K., Stayton, P.S., Hoffman, A.S., Wilson, M.R., 2003. Poly(2-alkylacrylic acid) polymers deliver molecules to the cytosol by pH-sensitive disruption of endosomal vesicles. Biochem. J. 372, 65–75.
Kharlampieva, E., Sukhishvili, S.A., 2003. Ionization and pH stability of multilayers formed by self-assembly of weak polyelectrolytes. Langmuir 19, 1235–1243.
Lichtenbeld, H.C., Yuan, F., Michel, C.C., Jain, R.K., 1996. Perfusion of single tumor microvessels: application to vascular permeability measurement. Microcirculation 3, 349–357.
Midoux, P., Monsigny, M., 1999. Efficient gene transfer by histidylated polylysine/pDNA complexes. Bioconjug. Chem. 10, 406–411.
Monsky, W.L., Fukumura, D., Gohongi, T., Ancukiewcz, M., Weich, H.A., Torchilin, V.P., Yuan, F., Jain, R.K., 1999. Augmentation of transvascular transport of macromolecules and nanoparticles in tumors using vascular endothelial growth factor. Cancer Res. 59, 4129–4135.
Ormai, S., Palkovits, M., 1975. Lymphocytosis induced by polymethacrylic acid. Dose-effect and toxicity. Blut 31, 239–246.
Oupicky, D., Ogris, M., Howard, K.A., Dash, P.R., Ulbrich, K.L., Seymour, W., 2002. Importance of lateral and steric stabilization of polyelectrolyte gene

delivery vectors for extended systemic circulation. Mol. Ther. 5, 463–472.
Rolland, A., Collet, B., Verge, R.Le, Toujas, L., 1989. Blood clearance and organ distribution of intravenously administered polymethacrylic nanoparticles in mice. J. Pharm. Sci. 78, 481–484.
Shan, S., Flowers, C., Peltz, C.D., Sweet, H., Maurer, N., Kwon, E.J., Krol, A., Yuan, F., Dewhirst, M.W., 2006. Preferential extravasation and accumulation of liposomal vincristine in tumor comparing to normal tissue enhances antitumor activity. Cancer Chemother. Pharmacol. 58, 245–255.
Sukhishvili, S., Granick, S., 2002. Layered, erasable polymer multilayers formed by hydrogen-bonded self-assembly. Macromolecules 35, 301–310.
Tozer, G.M., Prise, V.E., Wilson, J., Cemazar, M., Shan, S., Dewhirst, M.W., Barber, P.R., Vojnovic, B., Chaplin, D.J., 2001. Mechanisms associated with tumor vascular shut-down induced by combretastatin A-4 phosphate: intravital microscopy and measurement of vascular permeability. Cancer Res. 61, 6413–6422.
Trubetskoy, V.S., Wong, S.C., Subbotin, V., Budker, V.G., Loomis, A., Hagstrom, J.E., Wolff, J.A., 2003. Recharging cationic DNA complexes with highly charged polyanions for *in vitro* and *in vivo* gene delivery. Gene Ther. 10, 261–271.
Tseng, W.C., Jong, C.M., 2003. Improved stability of polycationic vector by dextran-grafted branched polyethylenimine. Biomacromolecules 4, 1277–1284.
Wu, N.Z., Klitzman, B., Rosner, G., Needham, D., Dewhirst, M.W., 1993. Measurement of material extravasation in microvascular networks using fluorescence video-microscopy. Microvasc. Res. 46, 231–253.
Wu, N.Z., Braun, R.D., Gaber, M.H., Lin, G.M., Ong, E.T., Shan, S., Papahadjopoulos, D., Dewhirst, M.W., 1997. Simultaneous measurement of liposome extravasation and content release in tumors. Microcirculation 4, 83–101.
Xie, A.F., Granick, S., 2002. Local electrostatics within a polyelectrolyte multilayer with embedded weak polyelectrolyte. Macromolecules 35, 1805–1813.
Yang, S.Y., Mendelsohn, J.D., Rubner, M.F., 2003. New class of ultrathin, highly cell-adhesion-resistant polyelectrolyte multilayers with micropatterning capabilities. Biomacromolecules 4, 987–994.
Yuan, F., Salehi, H.A., Boucher, Y., Vasthare, U.S., Tuma, R.F., Jain, R.K., 1994. Vascular permeability and microcirculation of gliomas and mammary carcinomas transplanted in rat and mouse cranial windows. Cancer Res. 54, 4564–4568.